Flower like Buffer Layer to Improve Efficiency of Submicron-Thick $CuIn_{1-x}Ga_xSe_2$ Solar Cells

Nae-Man Park, Dae-Hyung Cho, and Kyu-Seok Lee

In this article, a study of a flower like nanostructured CdS buffer layer for improving the performance of a submicron-thick $CuIn_{1-x}Ga_xSe_2$ (CIGS) solar cell (SC) is presented. Both its synthesis and properties are discussed in detail. The surface reflectance of the device is dramatically decreased. SCs with flower like nanostructured CdS buffer layers enhance short-circuit current density, fill factor, and open-circuit voltage. These enhancements contribute to an increase in power conversion efficiency of about 55% on average compared to SCs that don't have a flower like nanostructured CdS buffer layer, despite them both having the same CIGS light absorbing layer.

Keywords: $CuIn_{1-x}Ga_xSe_2$ (CIGS), flower like buffer layer, submicron-thick light absorber.

I. Introduction

As our consumption of fossil fuels increases, so too, in number, do our environmental and economic problems. Therefore, there is a great deal of interest in renewable energy sources that can create sustainable economic development. However, renewable energy sources cannot cost-efficiently satisfy the planet's vast energy consumption needs. Although solar energy is less cost effective than other power generation technologies, such as thermal, water, and nuclear power generation, it has received significant attention as a clean and unlimited energy source. To reduce the cost of power generation using solar radiation, intensive studies have focused on thin-film photovoltaic devices [1]–[2], of which $CuIn_{1-x}Ga_xSe_2$ (CIGS) solar cells (SCs) are the most promising as they have the highest power conversion efficiency (over 21%) [3] and good stability. This is significant because it opens up the possibility of silicon-like efficiency at low thin-film costs, which would then mean that we could achieve a sustainable $0.4/Watt. Many researchers have studied CIGS SCs using various methods, such as co-evaporation, sputtering, electro deposition, ink printing, and spray pyrolysis [4]–[6]. However, with regards to the aforementioned deposition processes, the normal thickness of a CIGS light absorbing layer is about 2 μm to 3 μm. To reduce the requirement for expensive material resources and production time, it is desirable to reduce the thickness of a CIGS light absorbing layer to the submicron level. This would lead to a low manufacturing cost. However, a thinner CIGS light absorbing layer is generally likely to show a lower conversion efficiency. Submicron-thick CIGS light-absorbing layers have been studied by several groups [7]–[11]. To achieve high conversion efficiency, they have tried to optimize the Ga content in a thin CIGS light-absorbing layer or

Manuscript received Feb. 5, 2015; revised July 15, 2015; accepted July 28, 2015.

This work was supported by Institute for Information & communications Technology Promotion (IITP) grant funded by the Korea government (MSIP) (B0101-15-0133, The core technology development of light and space adaptable energy-saving I/O platform for future advertising service).

Nae-Man Park (corresponding author, nmpark@etri.re.kr) is with the Information & Communications Core Technology Research Laboratory, ETRI, and also with the Department of Advanced Device Technology, UST, Daejeon, Rep. of Korea.

Dae-Hyung Cho (dhcho@etri.re.kr) is with the Information & Communications Core Technology Research Laboratory, ETRI, Daejeon, Rep. of Korea.

Kyu-Seok Lee (kyulee@etri.re.kr) is with the Technology Commercialization Division, ETRI, Daejeon, Rep. of Korea.

texturize the top surface of a transparent electrode with additional processes. From herein onwards, we present both the synthesis and the properties of a flower like nanostructured CdS buffer layer and an investigation of its properties. When this nanostructured buffer layer is adopted in submicron-thick CIGS SCs, the power conversion efficiency is increased by about 55% on average compared to SCs that don't have a flower like nanostructured CdS buffer layer, despite them both having the same CIGS light-absorbing layer.

II. Experiments

For our experiments, 800 nm thick CIGS films were grown on Mo/soda lime glass (SLG) through a three-stage process in which a sequence of In-Ga-Se/Cu-Se/In-Ga-Se co-evaporation was performed at substrate temperatures of 330°C (1st stage) and 570°C (2nd and 3rd stages). A 900 nm Mo film was deposited onto an SLG (25 mm × 25 mm × 1.1 mm polished glass) at a pressure of 2 mTorr at room temperature using a DC magnetron sputtering process at 300 W. For a normal sample, a CdS film was synthesized onto CIGS/Mo/SLG at 50°C in a bath; 0.015 M $CdSO_4$ and 56 ml of NH_4OH (28%) were put into the bath containing 300 ml of DI water. After 1 min, 0.75 M thiourea was added to the bath. Then, the reaction was carried out for 8 min. After completion of the procedure, the samples were washed with DI water and blow-dried using nitrogen gas. On the other hand, to synthesize the flower like nanostructured CdS film, all of 1.5 M $CdSO_4$, 1.5 M thiourea, and 65 ml of NH_4OH (28%) were added together to 370 ml of DI water at room temperature and the bath temperature was increased. In this case, the reaction time was 20 min to 25 min, at which the bath temperature was about 50°C. An ITO/non-doped ZnO window layer was deposited by radio-frequency magnetron sputtering using ZnO (99.9%, Cerac) and ITO (99.99%, In_2O_3:SnO_2 = 90:10) targets. A 70 nm-thick ZnO film was deposited in an Ar atmosphere with 25% O_2 at a pressure of 30 mTorr using a power of 400 W at ambient temperature. A 150 nm-thick ITO film was deposited in an Ar atmosphere of 50 mTorr with a power of 100 W at 200°C. An Al/Ni (3,000/50 nm) top grid contact was deposited by using an e-beam evaporator.

The final active region of the device was 0.47 cm^2. The power conversion efficiency (in-house active area efficiency) was measured using a solar simulator (Oriel 91193-1000) equipped with an AM 1.5 filter. Scanning electron microscopy (SEM) images were obtained using an FEI Sirion 400 operating at 10 keV to confirm the film thickness and the surface morphology. No metallic coating was carried out. To characterize the crystalline structure, X-ray diffraction (XRD) was performed using a Rigaku D/Max-RC Bede/DCC300 with Cu Kα (λ = 1.54 Å) radiation. XRD data was collected at 0.02 increments of 2θ at a scan rate of 3°/min with a θ-2θ goniometer and a sample rotation of 60 revolutions per minute. An ultraviolet/visible/near-infrared spectrophotometer (HITACHI U-4001) was used to observe the optical reflectance of the CdS surface, in which the film was synthesized on a Mo/SLG substrate, and the reference sample was Mo/SLG.

III. Results and Discussion

Figure 1 shows plane-view SEM images of CdS films. When the flower like nanostructured CdS film was synthesized, the flat CdS film was first deposited and then nanostructures were fabricated on the flat film (as is clearly shown in Fig. 1(b)). Unlike normal CdS film on a CIGS light-absorbing layer, flower like nanostructured CdS film has a complex surface morphology (see Figs. 1(c) and 1(d)). The flower like nanostructures on the CIGS/Mo/glass substrate stand closer together and more uniformly than those on a glass substrate (see Figs. 1(a) and 1(d)).

The crystalline structure of the flower like nanostructured CdS film is distinct from normal CdS film. A normal CdS film generally has (200), (110), and (112) crystal orientations in a hexagonal structure [12], as shown in Fig. 2(b). However, the flower like nanostructured CdS film has additional crystal orientations, such as (100), (102), and (004), in a hexagonal structure [13]. It also has (111) crystal orientation in a CdO cubic structure (see Fig. 2(a)) [14]. The reason that the flower like nanostructured CdS film has more crystal orientations than

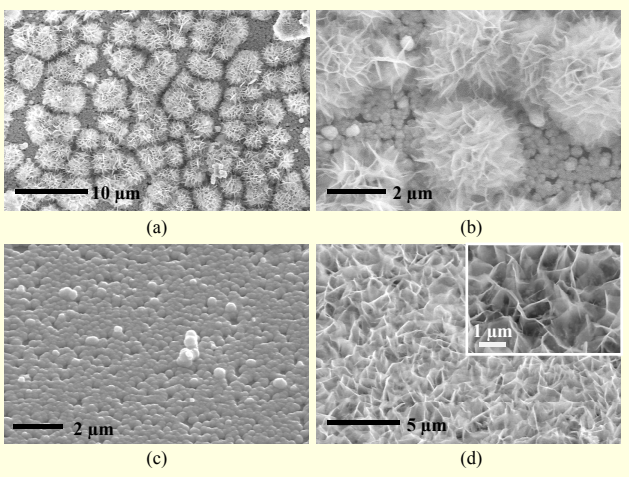

Fig. 1. Plane-view SEM images of CdS films synthesized on glass substrate ((a) and (b)) and CIGS/Mo/glass substrate ((c) and (d)); (c) is normal CdS film and (d) is flower like nanostructured CdS film. During synthesis of flower like nanostructured CdS, nanostructures were fabricated after flat CdS film was formed.

ETRI Journal, Volume 37, Number 6, December 2015
http://dx.doi.org/10.4218/etrij.15.0115.0114

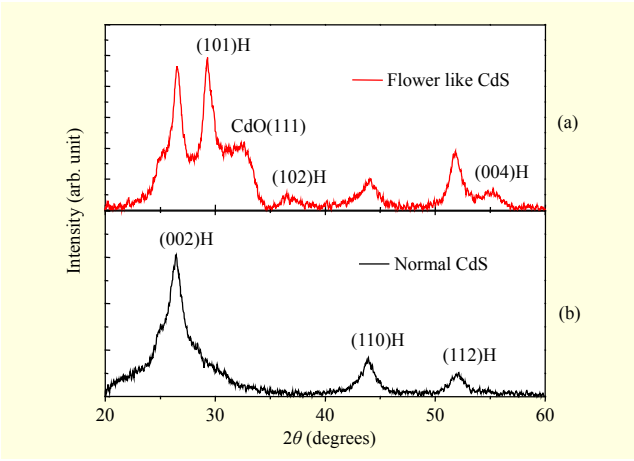

Fig. 2. XRD patterns collected from (a) flower like nanostructured CdS film and (b) normal CdS film deposited on glass. Flower like nanostructured CdS film has more complex crystalline structure.

normal film seems to be due to its complicated nanostructure networks. In chemical bath deposition, ions combine to form nuclei on the substrate as well as in solution. Precipitation occurs when the ionic products exceed the solubility product (that is, CdS) [15]. Film growth takes place via ion-by-ion condensation or adsorption of colloidal particles from the solution onto the substrate. Slow reaction generally shows adherent smooth films, but fast reaction increases the heterogeneity and leads to randomly oriented nanostructured films such as our flower like nanostructured CdS film.

Figure 3 shows a schematic diagram of the CIGS SC structure and cross-sectional SEM images of CIGS SCs with normal CdS film and the flower like nanostructured CdS film. Two SCs have different CdS films, but all other conditions are the same. A CIGS film of 800 nm as a light-absorbing layer was deposited on Mo film. As shown in Fig. 3, the SC surface is smooth in a normal device (see Fig. 3(b)), but it is complex in the SC with the flower like nanostructured CdS film (see Fig. 3(c)). The processed thickness of the ITO/ZnO window layer is about 220 nm. Therefore, the flat CdS film formed under the flower like CdS nanostructure is about 40 nm (see Fig. 3(c)), which is very similar to the thickness (approx. 50 nm) of normal CdS film synthesized by a normal process. As previously mentioned (see Fig. 1(b)), a 40 nm-thick flat-film was first deposited, and then nanostructures were fabricated on the flat film during the synthesis of the flower like nanostructured CdS film. Comparing Fig. 3(c) with the inset in Fig. 1(d), the wall thickness of the flower like CdS nanostructure also increased after the deposition of the ITO/ZnO window layer. Using these SC structures, we measured the device performance.

Figure 4 shows the number of devices in terms of efficiency, fill factor, open-circuit voltage (V_{oc}), and short-circuit current

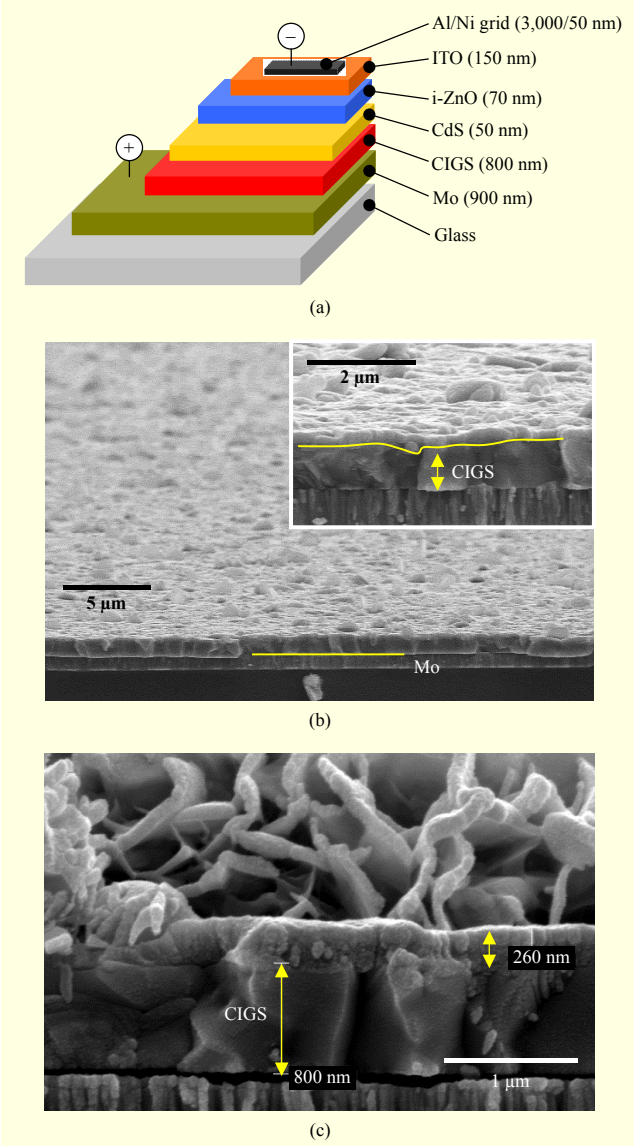

Fig. 3. (a) Schematic diagram of CIGS SC structure. Cross-sectional SEM images of CIGS SCs with (b) normal CdS film and (c) flower like nanostructured CdS film.

density (J_{sc}). When the flower like nanostructured CdS film was adopted in SCs, all parameters were improved. The average power conversion efficiency was increased by about 55% from 8.7% to 13.5%. Normally, a textured surface decreases the reflection of incident light and thereby increases of short-circuit current density in the SC, resulting in the increase an external quantum efficiency [10], [16]. In this study, this effect was confirmed. In Fig. 5(a), light reflectance is greatly decreased on the flower like nanostructured CdS film when comparing to normal CdS film in both structures of CdS single layer and ITO/ZnO/CdS multilayer, which results in the increase of external quantum efficiency in the SC with the flower like nanostructured CdS film [17]. Figure 5(b) shows

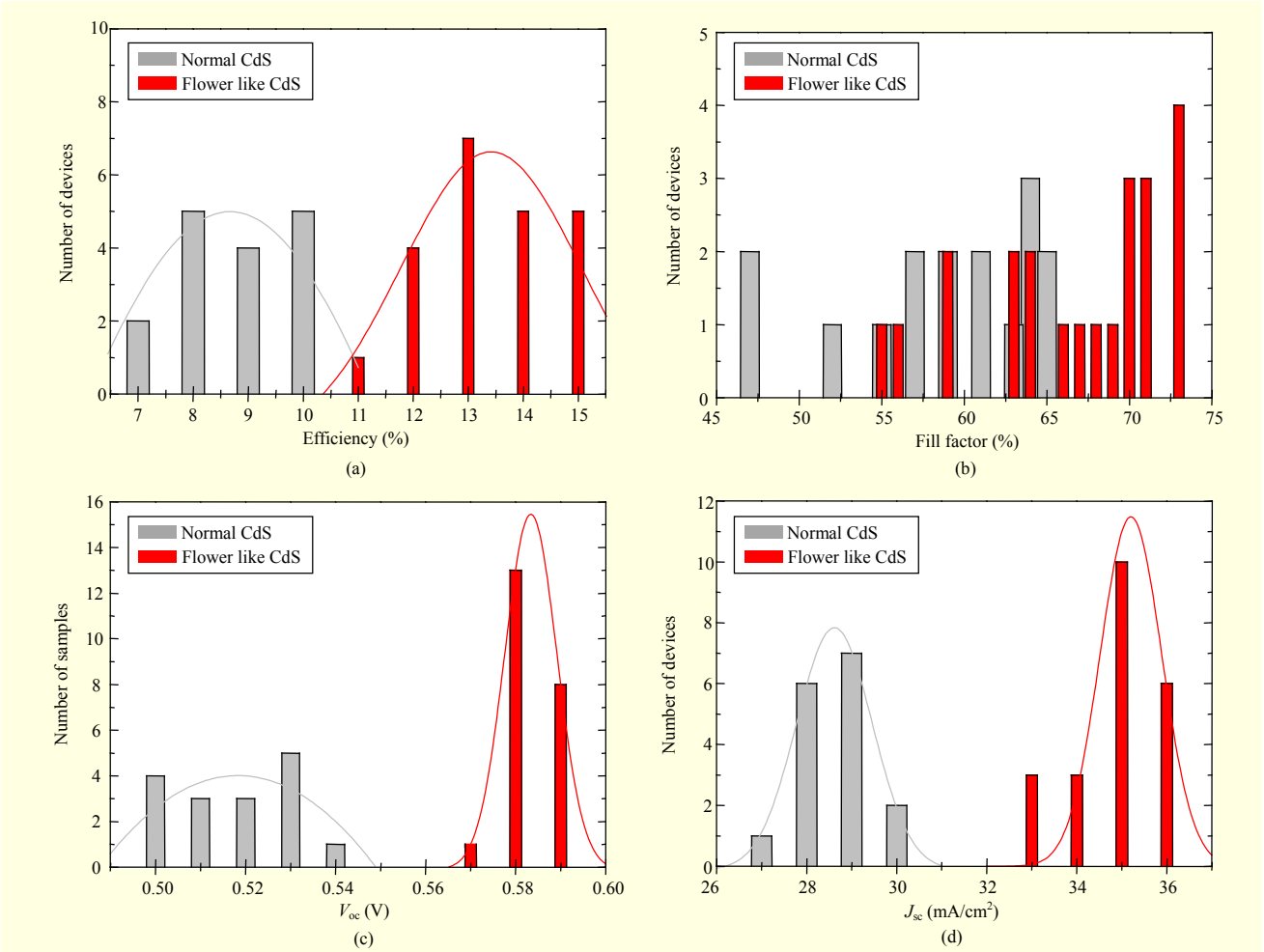

Fig. 4. CIGS solar cell performance in terms of (a) efficiency, (b) fill factor, (c) open-circuit voltage (V_{oc}), and (d) short-circuit current (J_{sc}). Red bars are data for flower like nanostructured CdS film, and gray bars are for normal CdS film.

the representative current–voltage curves of CIGS SCs with normal CdS film and the flower like nanostructured CdS film. When fitting these curves with a two-diode model [18], the shunt resistances are about 494 Ω and 5,980 Ω for the normal device and the nanostructured device, respectively. Shunt resistance is related to the leakage current; high shunt resistance indicates low leakage current, which results in high open-circuit voltage [19]–[20]. In our SCs with the flower like nanostructured CdS film, open-circuit voltage was increased in addition to short-circuit current density. As shown in Fig. 2(a), CdO phase was formed during the synthesis of the flower like nanostructured CdS film. This indicates that more oxygen participates in the synthesis of the flower like nanostructured CdS film than in the synthesis of normal CdS film. Oxygen is able to passivate the defects at CIGS grain boundaries more effectively than sulphur [20]. Therefore, this oxygen effect can result in high shunt resistance and increase open-circuit voltage. Fill factor is also larger on average in SCs with the flower like nanostructured CdS film than those with normal CdS film due to the improvement of shunt resistance. All these improvements increased the average power conversion efficiency by about 55%, even though the same CIGS light-absorbing layer was used. It should be noted that the series resistances of the devices are about 2.3 Ω and 4.0 Ω for the normal device and the nanostructured device, respectively. Higher series resistance of the nanostructured device could be due to the larger thickness of CdS layer compared to a normal device. Although a flower like nanostructured buffer layer is able to cause the discontinuous interface between the ITO/ZnO and a buffer layer, the SCs with a flower like nanostructured CdS buffer layer showed an improved performance without any more process or treatment.

IV. Conclusion

We synthesized a flower like nanostructured CdS film and

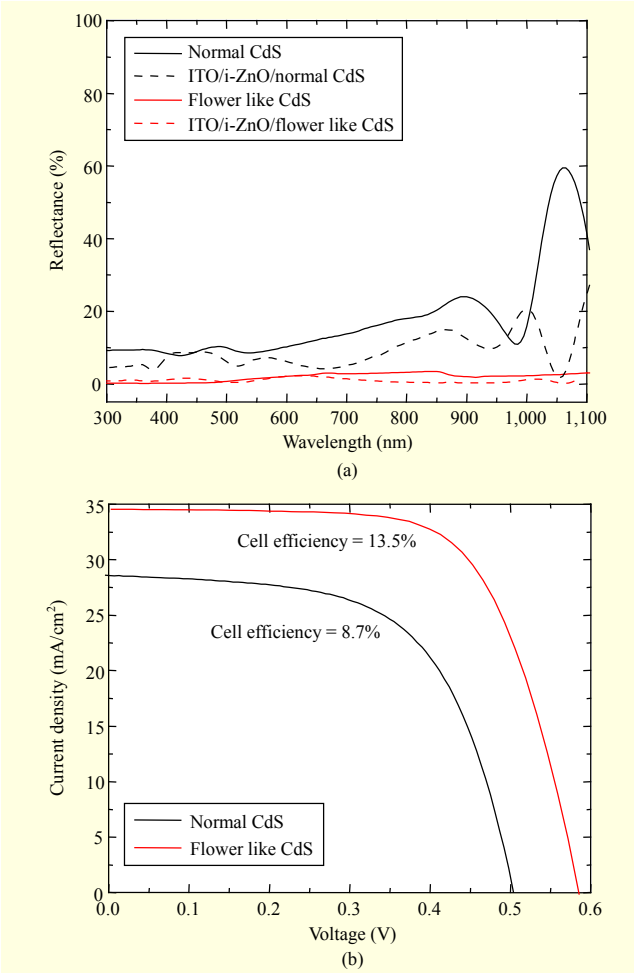

Fig. 5. (a) Surface reflectance of normal CdS and flower like nanostructured CdS films as function of optical wavelength; Mo/glass was used as substrate and reference sample for the reflectance measurement and (b) current density–voltage curves of CIGS SCs with average power conversion efficiency for both CdS films. Compared to normal device, performance of nanostructured device is dramatically improved.

applied it in submicron-thick CIGS SCs. The flower like nanostructured CdS film decreased the incident light reflection on the device surface as well as the leakage current. Therefore, the short-circuit current density, open-circuit voltage, and fill factor were all enhanced. As a result, the power conversion efficiency was dramatically increased by about 55% on average without any more process or treatment.

References

[1] M.A. Green, "Thin-Film Solar Cells: Review of Materials, Technologies, and Commercial Status," *J. Mater. Sci.*, vol. 18, no. 1, Oct. 2007, pp. 15–19.

[2] F.C. Krebs, "Fabrication and Processing of Polymer Solar Cells: A Review of Printing and Coating Techniques," *Solar Energy Mater. Solar Cells*, vol. 93, no. 4, Apr. 2009, pp. 394–412.

[3] P. Jackson et al., "Properties of Cu(In,Ga)Se_2 Solar Cells with New Record Efficiencies up to 21.7%," *Physica Status Solidi (RRL)*, vol. 9, no. 1, Jan. 2015, pp. 28–31.

[4] M. Kemell, M. Ritala, and M. Leskela, "Thin-Film Deposition Methods for $CuInSe_2$ Solar Cells," *Critical Rev. Solid State Mater. Sci.*, vol. 30, no. 1, Jan. 2005, pp. 1–31.

[5] T. Todorov and D.B. Mitzi, "Direct Liquid Coating of Chalcopyrite Light-Absorbing Layers for Photovoltaic Devices," *European J. Inorganic Chem.*, vol. 2010, no. 1, Jan. 2010, pp. 17–28.

[6] N.-M. Park, H.S. Lee, and J. Kim, "Reactive Sputtering Process for $CuIn_{1-x}Ga_xSe_2$ Thin-Film Solar Cells," *ETRI J.*, vol. 34, no. 5, Oct. 2012, pp. 779–782.

[7] K. Ramanathan et al., "Processing and Properties of Submicron CIGS Solar Cells," *World Conf. Photovoltaic Solar Energy Convers.*, HI, USA, May 7–12, 2006, pp. 380–383.

[8] N.-M. Park et al., "Effect of Se Flux on $CuIn_{1-x}Ga_xSe_2$ Film in Reactive Sputtering Process," *Progress Photovoltaic: Res. Appl.*, vol. 20, no. 7, Nov. 2012, pp. 899–903.

[9] S. Yang et al., "Bandgap Optimization of Submicron-Thick Cu(In,Ga)Se_2 Solar Cells," *Progress Photovoltaic: Res. Appl.*, vol. 23, no. 9, Sept. 2015, pp. 1157–1163.

[10] B. Hua et al., "Efficient Photon Management with Nanostructures for Photovoltaics," *Nanoscale*, vol. 5, no. 15, May 2013, pp. 6627–6640.

[11] M. Singh et al., "Thin-Film Copper Indium Gallium Selenide Solar Cell Based on Low-Temperature All-Printing Process," *ACS Appl. Mater. Interfaces*, vol. 6, no. 18, Sept. 2014, pp. 16297−16303.

[12] Y.-D. Chung et al., "Effect of Annealing on Cds/Cu(In,Ga)Se_2 Thin-Film Solar Cells," *Current Appl. Physics*, vol. 11, no. 1, Jan. 2011, pp. S65–S67.

[13] Y. Guo et al., "Facile Additive-Free Solvothermal Synthesis of Cadmium Sulfide Flower-Like Three Dimensional Assemblies with Unique Optical Properties and Photocatalytic Activity," *CrystEngComm*, vol. 13, no. 16, Aug. 2011, pp. 5045–5048.

[14] D.S. Dhawale et al., "Room Temperature Synthesis and Characterization of CdO Nanowires by Chemical Bath Deposition (CBD) Method," *Appl. Surface Sci.*, vol. 254, no. 11, Mar. 2008, pp. 3269–3273.

[15] R.S. Mane and C.D. Lokhande, "Chemical Deposition Method for Metal Chalcogenide Thin Films," *Mater. Chem. Physics*, vol. 65, no. 1, June 2000, pp. 1–31.

[16] Y.-K. Liao et al., "Non-antireflective Scheme for Efficiency Enhancement of Cu(In,Ga)Se_2 Nanotip Array Solar Cells," *ACS Nano*, vol. 7, no. 8, Aug. 2013, pp. 7318–7329.

[17] N.-M. Park et al., "Surface Texturing Effect of CdS Film on CIGS Solar Cell Efficiency," *Electrochem. Soc. Meeting*, Vienna,

Austria, Oct. 4–9, 2009, p. 757.
[18] K.-S. Lee et al., "Analysis of the Current-Voltage Curves of a Cu(In,Ga)Se_2 Thin-Film Solar Cell Measured at Different Irradiation Conditions," *J. Opt. Soc. Korea*, vol. 14, no. 4, Dec. 2010, pp. 321–325.
[19] A.D. Dhass, E. Natarajan, and L. Ponnusamy, "Influence of Shunt Resistance on the Performance of Solar Photovoltaic Cell," *Int. Conf. Emerging Trends Electr. Eng. Energy Manag.*, Chennai, India, Dec. 13–15, 2012, pp. 382–386.
[20] M. Mushrush et al., "Development of a High-Pressure CdS Sputtering Process for Improved Efficiency in CIGS-Based Photovoltaic Devices," *IEEE Photovoltaic Specialists Conf.*, Austin, TX, USA, June 3–8, 2012, pp. 895–898.

Nae-Man Park received his BS and MS degrees in physics from Hanyang University, Seoul, Rep. of Korea, in 1995 and 1997, respectively. He received his PhD degree in material science and engineering from Gwangju Institute of Science and Technology, Rep. of Korea, in 2002. Since 2002, he has been with ETRI, and more recently (2015), he has been working at the Department of Advanced Device Technology, University of Science and Technology, Daejeon, Rep. of Korea, where he is a professor. His research interests include nanomaterials and nanostructures, including QDs and nanowires. He has also been involved in research related to devices using nanomaterials or nanostructures, such as LEDs, solar cells, and transparent/stretchable electrodes.

Dae-Hyung Cho received his BS and MS degrees in electrical engineering from Korea University, Seoul, Rep. of Korea, in 2007 and 2009, respectively. Since 2009, he has been with ETRI, where he is now a researcher. He is carrying out research on the fabrication and characterization of Cu(In,Ga)Se2 thin-film solar cells. His research interests include the development of functional compound semiconductors and transparent conductive oxide materials for photovoltaic and electronic devices.

Kyu-Seok Lee received his BS and MS degrees from Yonsei University, Seoul, Rep. of Korea and his PhD degree from Northeastern University, Boston, MA, USA, all in physics, in 1979, 1981, and 1990, respectively. He was a research associate at Northeastern University in 1990 and spent his postdoctoral years of 1991–1992 at the Institute of Physical and Chemical Researches, Saitama, Japan. Since 1992, he has been with ETRI. His research interests include solid-state spectroscopy, physical phenomena in high magnetic fields, and the physics of semiconductor devices, such as light-emitting diodes, solar cells, laser diodes, and field-effect transistors.